Mechanics of Quantum-Dot Self-Organization by Epitaxial Growth on Small Areas

Robert V. Kukta
Associate Professor
Mem. ASME
Department of Mechanical Engineering,
State University of New York,
Stony Brook, NY 11794-2300
e-mail: robert.kukta@stonybrook.edu

Energetic arguments are used to understand the mechanics of Stranski–Krastanow epitaxial systems constrained to grow on a finite area of a substrate. Examples include selective area epitaxy and growth on patterned substrate features as raised mesa and etched pits. Accounting only for strain energy, (isotropic) surface energy, wetting layer potential energy, and geometric constraints, a rich behavior is obtained, whereby equilibrium configurations consist of a single island, multiple islands, or no islands, depending on the size of the growth area. It is shown that island formation is completely suppressed in the case of growth on a sufficiently small area. These behaviors are in stark contrast to growth on an indefinitely large area, where the same model suggests that the minimum free energy configuration of systems beyond the wetting layer transition thickness is a single island atop a wetting layer. The constraint of growing on a finite area can suppress island coarsening and produce minimum energy configurations with multiple self-organized islands of uniform size and shape. [DOI: 10.1115/1.4000903]

1 Introduction

The Stranski–Krastanow mode of epitaxial growth has been heavily studied over the past 20 yrs. with the goal of self-assembling nanostructures for electronic and optoelectronic applications. In this mode of growth, islands spontaneously assemble atop an initial wetting layer that covers the substrate. Islands can act as domains for quantum confinement (quantum dots), and if properly arranged, configurations of islands may serve as the building blocks for devices with exceptional characteristics. While the mechanics of island formation is well-known [1,2], the problem of self-organizing islands into regular patterns has been a challenge. One method of achieving self-organization that has shown promise is selective area epitaxy.

In selective area epitaxy, deposition of film material is isolated to certain areas of the substrate. This can be done by patterning features in a deposited mask [3–5] or by mechanically affixing a nanostencil to the substrate [6]. Both methods expose only the areas of the substrate, where deposition is to occur. Furthermore, mass transport is constrained to occur primarily within these areas. One can also confine mass transport to certain areas by depositing onto a topographical patterned substrate. For example there is a substantial activation barrier for material to diffuse from the top of a raised mesa [7] or out of a pit [8] etched into the substrate surface. Hence growth on patterned substrate features can be expected to have similar features to selective area epitaxy.

Growth on a confined area has been shown to be fundamentally different than growth on large unpatterned substrates. A key feature is that the number of islands that form can apparently be controlled by varying the size of the growth area [7,4,8]. The trend is that smaller areas tend to support fewer islands; however, this alone would not be important. The important feature is that the multiple island configurations that arise are often regularly arranged and exhibit uniform size and shape [7,8]. This implies a strong resistance to island coarsening, which is not observed in growth on unpatterned substrates. Resistance to coarsening and the corresponding ability to achieve regular and predictable arrays of islands is critical for the advancement of this technology. It is interesting to note that coarsening is also inhibited in a two-phase epitaxial monolayer, wherein the morphology is constrained to a plane. In the present case the morphology is three-dimensional and the constraint is lateral [9,10]. While the two systems are different, it is apparent that morphological constraints play important roles in coarsening.

Several theoretical and computational investigations have been done very recently to understand the mechanisms by which islands self-organize on patterned substrates [11–15]. All of these investigations focus on substrate topography as the driving force for organization, and no one has asked the basic question of whether or not the constraint of growing on a finite area has a role in organization. This question applies to growth within an open window of a mask, but also to cases of growth on raised mesas and within pits etched into the substrate surface. The goal of this work is to limit attention to the areal constraint and determine if that alone can provide an explanation for apparently stable configurations of multiple islands.

2 Model

There are three essential ingredients to the mechanics of island formation in Stranski–Krastanow systems. The first is the strain energy associated with a lattice mismatch between the deposited material and substrate. The strain energy of an island configuration is generally lower than an equivalent flat film configuration, and hence, strain energy drives island formation. On the other hand, surface energy (assumed isotropic) is minimum for the flat film configuration, and therefore, competes with the driving force for island formation. For an island of a given volume the relative magnitude of surface energy to strain energy determines the height to width aspect ratio of the island. High strain and low surface energies lead to a high aspect ratio, while low strain and high surface energies lead to a low aspect ratio. During Stranski–Krastanow growth, the first few monolayers of deposited material form a wetting layer on the substrate, and hence, a third ingredient is needed to inhibit island formation during the early stages of growth. This is typically introduced in the form of a wetting layer potential that penalizes roughness formation at locations where film thickness is small [1,16,17,15]. In terms of energy, the wetting layer potential is characterized by an additional film surface

Contributed by the Applied Mechanics Division of ASME for publication in the JOURNAL OF APPLIED MECHANICS. Manuscript received June 24, 2008; final manuscript received October 13, 2009; published online March 31, 2010. Assoc. Editor: Jian Cao.

energy that depends on the local thickness of the film. The additional energy becomes large as thickness tends to zero and decays monotonically with increasing thickness.

The wetting layer is taken to be of uniform thickness H. For simplicity an island is considered to be axisymmetric with its shape characterized by its radial size R and aspect ratio $a=h(0)/R$, such that the height of the island above the wetting layer is given by

$$h(r) = \frac{aR}{4}\left(1 - \frac{r^2}{R^2}\right)\left[4 + (4+\pi^2)\frac{r^2}{R^2}\right]\cos^2\left(\frac{\pi r}{2R}\right) \tag{1}$$

where r is the radial position. The height function $h(r)$ is chosen such that the island meets the wetting layer with zero slope, as is typical of islands with isotropic surface energy [1]. Furthermore, in order to limit the parameter space, curvatures at $r=0$ and $r=R$ are taken to vanish. According to Eq. (1), the volume of an island is given by

$$V_I = 1.18344aR^3 \tag{2}$$

The strain energy is calculated semi-analytically under the assumption of isotropic linear elasticity, where the island, wetting layer, and substrate are assumed to have the same elastic constants. The substrate is taken to be a half-space. It is noted that while islands are constrained to form on a finite area determined by an open window in a mask, the mask is assumed to have negligible stiffness and can therefore be neglected in the elastic boundary value problem. The film surface is traction-free and, relative to the substrate, the film material supports a homogeneous transformation strain ϵ_0, which accounts for the lattice mismatch. An approximation is made for small values of the aspect ratio. A first-order approximation is found to miss necessary features, and therefore, a second-order approximation is obtained following the method outline elsewhere [18,11]. In the case of no wetting layer ($H=0$), the total strain energy of a single island system is

$$U_I = V_I M\epsilon_0^2\left[1 - 1.67425(1+\nu)a + \frac{3.04705(1+\nu)(0.87879-\nu)(2.01847+\nu)}{1-\nu}a^2\right] \tag{3}$$

where $M=2G(1+\nu)/(1-\nu)$ is the film modulus, ν is Poisson's ratio, and G is shear modulus. In Eq. (3), the first term in the square bracket is due solely to the mismatch strain, while the second and third terms are the first and second-order corrections of the energy associated with the island geometry, respectively. The raised nature of an island allows for relaxation of a portion of the mismatch strain, thereby reducing the strain energy of the island relative to an equivalent flat film. Note that the first-order correction (second term) is negative definite for all physically meaningful values of ν (in the range of $-1<\nu\leq(1/2)$), while the second-order correction (third term) is positive definite. This indicates that the driving force for an island to increase in aspect ratio decreases with increasing aspect ratio, which is missed by the first-order approximation.

The addition of a wetting layer of thickness H over area A of the substrate adds strain energy

$$U_w = AHM\epsilon_0^2 \tag{4}$$

to the system. In order to limit the parameter space of this investigation, the energies associated with the wetting layer boundary, where it meets the mask, are omitted. A typical wetting layer is only a few monolayers in thickness. Hence the boundary should be treated as an atomic scale step rather than a continuum level boundary [18,19]. Energies associated with the boundary include the partial relaxation of mismatch strain near the boundary and a step edge excess energy. Both of these energies require additional constitutive parameters, and to avoid obfuscating the basic result with additional parameters, it is assumed that these energies offset each other; in other words, it is assumed that the energy reduction due to strain relaxation equals the increase associated with step edge excess energy. Detailed consideration for these energies may have significant effect, depending on the specific material system, and should be addressed in future work.

The surface energy per unit area of the film surface is taken to be a constant γ. In the case of a flat film of area A, the total film surface energy is

$$\Gamma_0 = \gamma A \tag{5}$$

Introduction of an island adds surface energy

$$\Gamma_I = 3.07842a^2R^2\gamma \tag{6}$$

which is an approximation for small values of a, consistent with Eq. (3). This energy is positive definite, and therefore, acts as a penalty against the formation of islands. One should note that it represents the first-order effect of the island shape, similar to the second term in Eq. (3); both scale as a^2, considering that V_I in Eq. (3) scales with a. The second-order correction to Eq. (6) vanishes.

The wetting layer potential energy acts to modify the surface energy such that the penalty against island formation is increased for relatively thin films, where the notion of "thin" is defined by a material length parameter l. The potential energy for a flat film of area A and thickness H is modeled as

$$\Gamma_{w0} = \gamma_w A e^{-H/l} \tag{7}$$

where γ_w is an energy per unit area. This term effectively increases surface energy by the amount of γ_w for $H=0$ and decays as H becomes large compared with l. An island adds energy

$$\Gamma_{wI} = -\gamma_w \pi R^2 e^{-H/l} + \int_{S_I} \gamma_w e^{-(H+h)/l} dS \tag{8}$$

to the total wetting later potential energy, where S_I denotes the surface of the island. Equation (8) replaces the energy associated with the island's footprint (first term) by that of the island's surface (second term). Maintaining the current second-order approximation in the aspect ratio, Eq. (8) can be written as

$$\Gamma_{wI} = \gamma_w \pi R^2 e^{-H/l} f(a, aR/l) \tag{9}$$

where

$$f(a, aR/l) = \frac{1}{R^2}\int_0^R e^{-h(r)/l}[2 + h'(r)^2] r dr - 1 \tag{10}$$

is a dimensionless function of dimensionless variables a and aR/l. It is noted that the exponential in Eq. (10) is not approximated because the exponent $-h(r)/l$ scales as aR/l and the ratio l/R may be similar to or even smaller than a.

The total free energy of a system with n islands is given by

$$\mathcal{F} = n(U_I + \Gamma_I + \Gamma_{wI}) + U_w + \Gamma_0 + \Gamma_{w0} + U_{II}^n \tag{11}$$

where U_{II}^n is added to account for the elastic interaction energy between islands. A general semi-analytical result for the second-order approximation of U_{II}^n is difficult to obtain. Therefore, the system is first studied in general with the interaction energy neglected, and later, a specific case is considered to weigh the effect of the interaction energy.

3 Analysis

In the case of an unbounded deposition area ($A\to\infty$), the model described in Sec. 2 predicts that a single island configuration is always lower in free energy than an equivalent system with more than one island. The current understanding is that additional physics, such as faceting, is needed to stabilize a multiple island configuration [20,16]. However, it is demonstrated here that constraining deposition to a finite area might also stabilize a multiple number of islands.

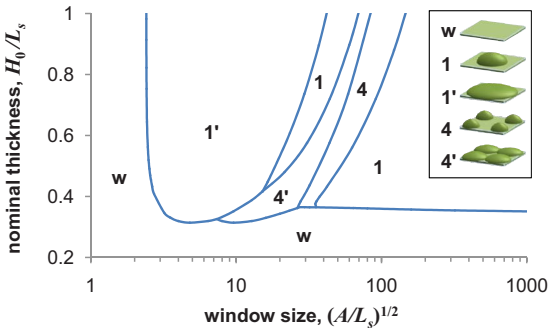

Fig. 1 Plot of the minimum energy configuration as a function of window size and nominal film thickness for the case $\nu=0.3$, $\bar{l}=0.1$, and $\bar{\gamma}_w=0.5$. The elastic interaction energy between islands is neglected.

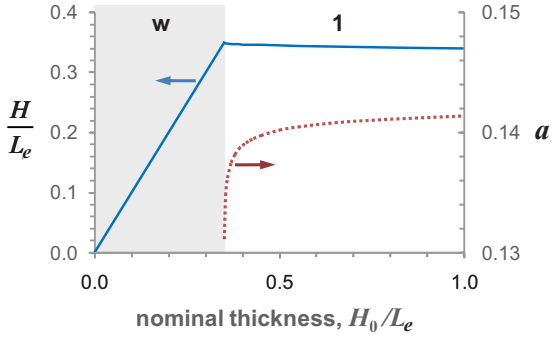

Fig. 2 Plot of the wetting layer thickness and island aspect ratio of the minimum energy configuration versus nominal film thickness for the case of window size $(A/L_e^2)^{1/2}=1000$ and the same material constants as in Fig. 1

For square windows of area A, minimum energy configurations are calculated for a given volume of deposited material. As the purpose of this article is only to introduce the idea that window size affects the minimum energy configuration, attention is limited to one-island and four-island configurations because these are expected to be the most prominent. In the four-island case, the islands are assumed to be of the same size and shape and are located at the corners of the square window. The total volume of material deposited in the window is given by

$$V_T = nV_I + AH = AH_0 \tag{12}$$

where n is the number of islands, V_I is the volume an island (Eq. (2)), and H is the wetting layer thickness. It is convenient to represent the deposited volume in terms of the nominal film thickness H_0, which is the thickness of a flat film of the same volume.

For a given area A and nominal thickness H_0, the configuration is defined by the number of islands (1 or 4), aspect ratio a, footprint radius R of the island(s), and wetting layer thickness H. In addition to these geometrical variables, the system is determined by the material constants ϵ_0, M, ν, γ, γ_w and l. The parameter space is reduced considerably by rewriting energy in the dimensionless form

$$\bar{\mathcal{F}} = \frac{\mathcal{F}}{\gamma L_e^2} = \bar{\mathcal{F}}(\bar{H}, \bar{R}, n; \bar{A}, \bar{H}_0, \bar{l}, \bar{\gamma}_w, \nu) \tag{13}$$

where

$$L_e = \frac{\gamma}{M\epsilon_0^2} \tag{14}$$

is the epitaxial length scale. The dimensionless energy is a function of the dimensionless configurational variables $\bar{H}=H/L_e$, $\bar{R}=R/L_e$, and n, and a function of the dimensionless system constants $\bar{A}=A/L_e^2$, $\bar{H}_0=H_0/L_e$, $\bar{l}=l/L_e$, $\bar{\gamma}_w=\gamma_w/\gamma$, and ν. Certain physical constraints must be imposed on the configuration. First, the wetting layer thickness is bounded by $0\leq\bar{H}\leq 1$, which excludes a negative thickness and provides that no more than the entire volume is contained in the wetting layer. Additionally the island footprint radius must be nonnegative and is also limited such that the island(s) fit completely within the growth window; therefore, $0\leq\bar{R}\leq m_n\bar{A}^{1/2}$, where $m_n=1/2$ for $n=1$ (one island) and $m_n=1/4$ for $n=4$ (four islands).

4 Results and Discussion

Figure 1 plots minimum energy configuration versus nominal film thickness $\bar{H}_0=H_0/L_e$ and window size $\bar{A}^{1/2}=(A/L_e^2)^{1/2}$ for a typical Poisson's ratio of $\nu=0.3$. The wetting constants were chosen somewhat arbitrarily as $\bar{l}=l/L_e=0.1$ and $\bar{\gamma}_w=\gamma_w/\gamma=0.5$. These constants might be determined empirically based on the salient features in Fig. 1; however, expected order-of-magnitude values are sufficient for the present discussion. Similar features are observed for a wide range of values of $\bar{l}$ and $\bar{\gamma}_w$.

For a fixed window size, Fig. 1 displays the result of equilibrium film growth following an increase in the nominal thickness. The initial deposition forms a wetting layer with no islands, as typical of Stranski–Krastanow growth, and provided that the window size is large enough, greater than about $(A/L_e^2)^{1/2}=2.4$, a critical thickness is reached where islands first become energetically favorable. Over a wide range of window sizes, the critical thickness is fairly uniform ranging between $H_0/L_e=0.32$ and 0.36. Wetting parameters were not refined to provide physically reasonable results; however, it is instructive to provide a physical estimate of this thickness. Taking the film modulus $M=180$ GPa, surface energy $\gamma=1$ J/m^2, and mismatch $\epsilon_0=4\%$, which are reasonable values for Ge, Si, or a similar semiconductor material system, the epitaxial length scale is calculated as $L_e=3.5$ nm. This implies a critical thickness for islanding in the range of $H_0=1.12$ nm-1.26 nm, which corresponds to a few monolayers of growth. The thickness can be adjusted to match the experimental values by altering the parameters l and γ_w.

For a relatively large window size, the wetting layer thickness maintains a fairly uniform thickness for subsequent growth after the formation of an island. This is illustrated in Fig. 2, which the plots wetting layer thickness H/L_e versus deposition amount for a window size of $(A/L_e^2)^{1/2}=1000$. Up to about $H_0/L_e=0.35$, no islands are present and the wetting layer thickness increases linearly with the deposition thickness. After $H_0/L_e=0.35$, all subsequent deposition is collected into a single island. Additionally, a modest amount of material in the wetting layer is also transferred to the island, as the wetting layer thickness is shown to decrease slightly with the deposition amount. Observe that for large windows, as in Fig. 2, a single large island is always favored over multiple smaller islands. Provided that a kinetic pathway exists, many small islands will tend to coarsen into fewer larger islands and ultimately into a single island. This context is the basis for the current understanding of epitaxial systems. However, as apparent in Fig. 1, growth on a window of finite size exhibits a much richer behavior.

For relatively small window sizes, the critical thickness for island formation is substantially increased beyond that of growth on a large area. This corresponds to the anomalous critical thickness for the onset of three-dimensional island nucleation observed recently in the experiments of Cojocaru et al. [6]. In the extreme case of a small window size, islanding is found to be suppressed. For the range of nominal thicknesses plotted in Fig. 1, islanding is completely suppressed for growth on windows less than $(A/L_e^2)^{1/2}=2.4$. For the physical example used previously, wherein

L_e=3.5 nm, this amounts to a square window with a side length of 8.4 nm. Arguably, this is too small to claim quantitative accuracy, but qualitatively, one might expect windows smaller than a critical size to inhibit island formation. To explain this, it is first necessary to understand that an island of a given volume has a preferred (minimum energy) shape that is roughly independent of the wetting layer thickness. Neglecting the effect of the wetting layer potential (Eq. (9)), the energy associated with an island is given by $\mathcal{F}_I = U_I + \Gamma_I$. Using Eq. (2) and minimizing $\mathcal{F}_I$ for fixed island volume V_I provides the equilibrium aspect ratio as the solution to

$$3.66862a^{1/3} = \frac{V_I^{1/3}}{L_e}\left[1.67425(1+\nu) - \frac{6.0941(1+\nu)(0.87879-\nu)(2.01847+\nu)}{1-\nu}a\right] \tag{15}$$

which is readily plotted by calculating $V_I^{1/3}/L_e$ for a range of a. From the aspect ratio, the radius R is determined by Eq. (2). The aspect ratio begins at $a=0$ for an island of infinitesimal volume and then increases with increasing volume until it asymptotes to the value $a=0.2747(1-\nu)/(0.87879-\nu)(2.01847+\nu)$ and grows with a fixed aspect ratio, similar to the plot in Fig. 2. The island radius, however, begins at a finite value for an island of infinitesimal volume and grows monotonically with increasing volume. For the case of $\nu=0.3$, an island of infinitesimal volume forms with radius $R/L_e \approx 1.5935$. This implies that when the side length of the window is less than $(A/L_e^2)^{1/2}=3.187$, there is an energetic penalty due to the constraint imposed on the island by the window; the island must form with a smaller radius and higher aspect ratio than it would prefer in the absence of the constraint. As the island grows in volume, the magnitude of this penalty increases. Furthermore, the preferred radius of the island also increases so that larger windows impose a radial constraint on larger islands. Configuration (1′) in Fig. 1 is used to denote an island that fills the entire window and is therefore unable to expand radially. Configuration (1) denotes the case of a single island that does not fill the entire window.

The minimum energy shape of an island is determined from a competition between the strain and surface energies. As an island's aspect ratio is increased beyond its preferred value, strain energy decreases while surface energy increases, and the net result is an increase in the total free energy. If the aspect ratio is sufficiently larger than its preferred value, the surface energy penalty can grow to a magnitude large enough for the free energy of the island configuration to exceed that of a flat film. This occurs irrespective of the nature of the wetting layer potential. To illustrate, consider an island that fills the entire window (radius $R=(1/2)A^{1/2}$) and take the volume of the island to be AH_0 such that there is no wetting layer. Neglecting the wetting layer potential, compare the free energy of this configuration to that of a flat (wetting) layer of the same volume. Using the energies given in Sec. 2, it is calculated that a flat layer has the lower energy for windows sizes less than

$$\frac{A^{1/2}}{L_e} < \frac{3.10738}{1+\nu} + \frac{12.3029(0.87879-\nu)(2.01847+\nu)H_0}{(1-\nu)L_e} \tag{16}$$

The condition shown in Fig. 1 is less severe because the material can be shared between the island and wetting layer. However, taking $\nu=0.3$ and $H_0 \to 0$ suggests that windows of size $(A/L_e^2)^{1/2} < 2.4$ cannot support island formation, which is in agreement with the apparent asymptote that bounds the flat wetting layer configuration (w) and the single island configuration (1′) in Fig. 1.

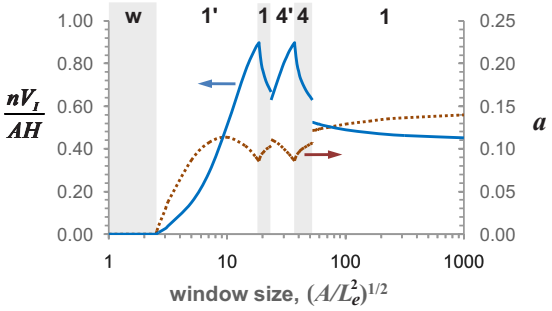

Fig. 3 Plot of the geometry of the minimum energy configuration versus window size at nominal film thickness H_0/L_e=0.5 and the same material constants as in Fig. 1. Geometry is represented in terms of the ratio of material volume in the island(s) to the wetting layer nV_I/AH and island aspect ratio a.

More generally, the penalty associated with the radial constraint on an island will cause the island to expel material to the wetting layer before it completely disappears (or cannot form to begin with). This is illustrated in Fig. 3, which plots the geometry of the minimum energy configuration versus the window size for a fixed nominal film thickness of H_0/L_e=0.5. The solid line plots the ratio of material volume in island(s) to that in the wetting layer. The single island configuration (1′) and four-island configuration (4′) correspond to cases where the islands fill the entire window and are therefore constrained from increasing further in radius. For both of these configurations, the fraction of the material in the wetting layer is shown to increase as the window size decreases. The penalty associated with increasing the aspect ratio of an island over its preferred level is moderated by a decrease in the island volume and a corresponding increase in the wetting layer thickness. This is in direct contrast to configurations (1) and (4), wherein islands do not fill the entire window and are free to grow radially in size. As window size is decreased for these configurations, the fraction of material in the island(s) increases. This occurs because the wetting layer thickness is approximately unchanged as the window size decreases and the excess wetting layer material (volume ΔAH, where ΔA is the change in the window area) is accommodated by the island(s). As the window area decreases the islands grow in volume and in radius until they reach the constraint imposed by the window. At that point, configuration (1) becomes (1′) and configuration (4) becomes (4′).

Figure 4 also illustrates the penalty associated with the radial constraint on an island, but in the context of material deposition on a window of fixed size. The wetting layer grows linearly with deposition thickness until configuration (4′) becomes the mini-

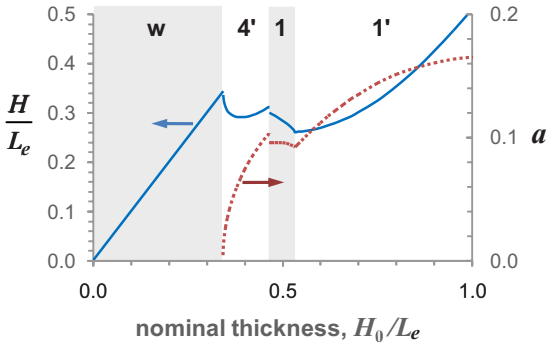

Fig. 4 Plot of the wetting layer thickness and island aspect ratio of the minimum energy configuration versus nominal film thickness for the case of window size $(A/L_e^2)^{1/2}$=20 and the same material constants as in Fig. 1

mum energy state. Subsequently configurations (1) and then (1′) become the minimum energy state with further growth. Observe that at $H_0/L_e=1$ the wetting layer increases in thickness at almost the same rate as configuration (w). This indicates that most of the deposited material gathers in the wetting layer, which occurs to offset the penalty of increasing the island's aspect ratio. A similar trend occurs toward the right side of (4′), while in the case of configuration (1), all of the deposited materials and a portion of the wetting layer material are accommodated by the island.

The fact that a four-island configuration can be of lower energy than a single island configuration is the result of the competition for material between the wetting layer and islands. Consider the transformation that occurs at $(A/L_e^2)^{1/2}\approx 53$ in Fig. 3, from configurations (1) to (4). Observe that at the point of this transformation, configuration (4) has more materials associated with the islands than configuration (1). Hence, one cannot directly compare the energies nor model the transformation without accounting for the material in the wetting layer. However, assume that there is no wetting layer and ignore the wetting layer potential; it is readily shown from the energies of Sec. 2 that the free energy of four islands is always larger than that of a single island of the same total volume. It is also found that the energy per unit volume of an (unconstrained) island tends to decrease as island volume increases. Hence the relative increase in the free energy in the transformation from a single island to four islands is moderated by an increase in the total material volume in the islands. It is further moderated by the wetting layer potential energy (Eq. (8)) associated with the islands. Consider, for example, an island shaped as a flat disk, such that $h(r)=h_0$, where h_0 is a constant. In this case, Eq. (8) becomes

$$\Gamma_{wI} = -\gamma_w \pi R^2 e^{-H/l}(1 - e^{-h_0/l}) \tag{17}$$

which acts to reduce the free energy by an amount proportional to substrate area πR^2 covered by the island. Since the substrate area covered by the islands tends to be larger in the case of multiple islands (consider a single hemispherical island versus four of the same total volume), this term will typically favor multiple islands. Additionally, the thickness of the wetting contributes to the appearance of multiple island configurations as a minimum energy state. The elastic energy (Eq. (4)) of the wetting layer decreases linearly as thickness decreases while the surface potential energy (Eq. (7)) increases exponentially as thickness decreases. Provided that the wetting layer is of sufficient thickness (compared with l), the energy associated with the wetting layer will be dominated by the elastic contribution and will decrease as the wetting layer thickness decreases. This is found to be the case for the transformation in Fig. 3 at $(A/L_e^2)^{1/2}\approx 53$. Both the reduction in the wetting layer thickness and increase in the island material from configurations (1) to (4) contribute to the transformation.

To further understand how a multiple island configuration can more stable than a single island, consider the case of no areal constraint. For an unconstrained system, the wetting layer comprises a substantial part of the total free energy, and hence, the wetting layer thickness is determined independently of the islands, which contribute a much smaller energy. The islands and wetting layer do not compete for the material except perhaps at regions very close to an island, where, in both simulations [21,16] and experiments [22], the wetting layer has been observed to be thinner; trenches form around an island's perimeter. In the case of a finite area, the island energy and wetting layer energy become comparable; the islands are then able to compete more effectively for the material. Considering the tendency of trench formation, one would expect systems with a larger total perimeter of the islands to have a lower nominal wetting layer thickness. This is apparent in Fig. 4, as more material is in the islands of the four-island configuration (4) than the one-island configuration (1). The four-island configuration becomes favored over the single island case because the total volume of the material in the islands is

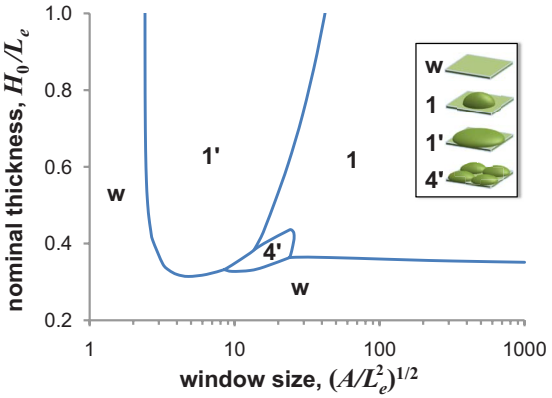

Fig. 5 Plot of the minimum energy configuration as a function of the window size and nominal film thickness for the case $\nu=0.3$, $\bar{l}=0.1$, and $\bar{\gamma}_w=0.5$, and with elastic interaction energy included. Configuration (4) was not considered in the calculation.

significantly larger, which is only possible on a finite area. This provides for a greater relaxation of the mismatch strain, and hence, a lower total strain energy.

At this point it should be noted that the model adopts a rather nonchalant continuum viewpoint of the wetting layer thickness, whereas it would be more appropriate to admit only discrete thicknesses as integer multiples of a monolayer thickness. Further work along these lines should certainly be pursued; however, the continuum assumption is not as severe as one might argue. On the length scale of this model, there is in fact a continuous reservoir for material in the form of adsorbed atoms (adatoms) atop the wetting layer. If one were to alter this model to admit only discrete wetting layer thicknesses, it would likely prove important to include an adatom phase to account for a incomplete monolayer. In this context, the current model simply adopts the same constitutive behavior for the wetting layer and adatom phases. A more general model can certainly be built to differentiate the two phases.

Up to this point the elastic interaction energy between islands has been neglected and its significance needs to be assessed. Island-island interactions occur only in the case of multiple islands, and therefore, only the four-island configurations need to be reconsidered. The elastic interaction acts to increase the free energy, and therefore, the question remains if a four-island configuration can actually be of lower energy than a single-island configuration. An analytical expression for the interaction energy is important to make the energy minimization analysis tractable. Even with the current reduced parameter system, the interaction energy depend on the volume of the islands, their aspect ratio, and separation distance. Furthermore is it important to maintain the same order of approximation to avoid extraneous behaviors. As the goal is only to determine if the four-island configuration persists as a minimum energy state, it is sufficient to limit attention to the (4′) configuration, where islands are in contact with each other. In this case the energy depends only on the island volume and aspect ratio. From the second-order approximation of the elastic field (which is itself affected by the interaction between the islands), the interaction energy between the two islands in contact and of the same size and shape is calculated as

$$U'_{II} = V_I M \epsilon_0^2 (1+\nu) a[0.1027 - 0.2080(0.9337+\nu)a] \tag{18}$$

Accounting for the nearest neighbor interactions, the total interaction energy for the (4′) configuration is approximated as $U_{II}^{4'}=4U'_{II}$. Including this result in the total free energy (Eq. (11)), Fig. 1, with configuration (4) omitted, is recalculated as Fig. 5. The effect of the interaction energy is substantial for large window sizes and large nominal thicknesses. The appearance of the (4′)

configuration is completely suppressed for $(A/L_e^2)^{1/2} > 26$. Recalling the example $L_e = 3.5$ nm, this corresponds to windows of side length larger than 90 nm. Differences between Figs. 1 and 5 are modest for window sizes less than about $(A/L_e^2)^{1/2} = 20$ mm or 70 nm using the example system. Additionally, the evolution of geometry for deposition on a window of size $(A/L_e^2)^{1/2} = 20$ is quite similar to Fig. 4, to the extent that including the result would be redundant. The main difference is that the (4′)-(1) transition occurs at approximately $H_0/L_e = 0.42$ rather than 0.45. As one might suppose by visually extrapolating the curves in Fig. 4, the (4′) to (1) transformation occurs with a slight increase in the wetting layer thickness and island aspect ratio when interaction energy is included, rather than the opposite effect when it is omitted. However, details such as this likely depend more on the choice of system parameters rather than island interactions. The important observation is that the island interaction energy does not eliminate the four-island configuration as a minimum energy state.

Finally, it is important to note that this analysis addresses minimum energy configurations without consideration for whether or not a particular transformation can occur. For a transformation to occur, an activation energy may be needed and there must be a viable kinetic pathway for it to follow. Observe that for certain transformations in Figs. 2 and 4, the change in geometry is continuous or nearly continuous, whereas others occur as abrupt changes. Nearly continuous changes such as the (w) to (1) transformation in Fig. 2, and (w) to (4′) and (1) to (1′) transformations in Fig. 4 should occur with little or no activation barrier. Hence, kinetics will likely have little effect on the these transformations, provided that the deposition rate is sufficiently low. The transformation from (4′) to (1) in Fig. 4, on the other hand, comes with a substantial change in geometry. Not only must the wetting layer thickness change, but four islands must spontaneously transform into a single island. This might come with a substantial activation barrier that would extend the prevalence of the (4′) configuration to much larger deposition amounts than predicted by the current equilibrium analysis. The pathway by which the transformation occurs would have to be determined in order to address this, which is a subject for future work.

5 Conclusions

Simple energetic arguments suggest a rather rich behavior of Stranski–Krastanow systems constrained to grow on a finite area of a substrate. Accounting only for the strain, (isotropic) surface, and wetting layer potential energies, it is found that the effect of a finite area can cause a configuration with multiple islands to be energetically favored over that of a single large island. This results from a complex competition between the various energy contributions as discussed above; however, a key observation is that the wetting layer may act as a source or sink of material for the islands. It is insufficient to compare the energies of the islands with the same total volume, as the ratio of the material in the wetting layer to the material in the islands depends on the growth area and also on the deposition amount. The analysis also suggests that there is a critical area size below which no islands will form.

Several extensions to this work are warranted. First only one- and four-island configurations were considered because they were expected to be the predominant ones. Preliminary calculations suggest that other configurations can occur as minimum energy states and the full configuration phase diagram should be obtained. Additionally the effect of the wetting layer boundary should be addressed as discussed previously. This will introduce additional constitutive parameters that may have significance, depending on the particular material system. As also discussed previously, work should be done to depart from the model of a continuously varying wetting layer thickness to one that considers discrete monolayers with the addition of an adatom phase to serve a continuous source and sink for material. Finally, kinetics is expected to play an important role in determining the configuration resulting from deposition. Issues that need to be addressed include the effect of deposition rate and possible activation barriers for certain transformations.

Acknowledgment

Research support for this work from the National Science Foundation through Grant No. CMS-0134123 is gratefully acknowledged.

References

[1] Kukta, R. V., and Freund, L. B., 1997, "Minimum Energy Configuration of Epitaxial Material Clusters on a Lattice-Mismatched Substrate," J. Mech. Phys. Solids, **45**(11–12), pp. 1835–1860.
[2] Johnson, H. T., and Freund, L. B., 1997, "Mechanics of Coherent and Dislocated Island Morphologies in Strained Epitaxial Material Systems," J. Appl. Phys., **81**, pp. 6081–6090.
[3] Lee, S. C., Stintz, A., and Brueck, S. R. J., 2002, "Nanoscale Limited Area Growth of InAs Islands on GaAs(001) by Molecular Beam Epitaxy," J. Appl. Phys., **91**, pp. 3282–3288.
[4] Vescan, L., Stoica, T., Hollander, B., Nassiopoulou, A., Olzierski, A., Raptis, I., and Sutter, E., 2003, "Self-Assembling of Ge on Finite Si(001) Areas Comparable With the Island Size," Appl. Phys. Lett., **82**, pp. 3517–3519.
[5] Yoon, T.-S., Zhao, Z., Liu, J., Xie, Y.-H., Ryu, D. Y., Russell, T. P., Kim, H.-M., and Kim, K.-B., 2006, "Selective Growth of Ge Islands on Nanometer-Scale Patterned SiO_2/Si Substrate by Molecular Beam Epitaxy," Appl. Phys. Lett., **89**, p. 063107.
[6] Cojocaru, C. V., Bernardi, A., Reparaz, J. S., Alonso, M. I., MacLeod, J. M., Harnagea, C., and Rosei, F., 2007, "Site-Controlled Growth of Ge Nanostructures on Si(100) via Pulsed Laser Deposition Nanostenciling," Appl. Phys. Lett., **91**, p. 113112.
[7] Kitajima, T., Liu, B., and Leone, S. R., 2002, "Two-Dimensional Periodic Alignment of Self-Assembled Ge Islands on Patterned Si(001) Surfaces," Appl. Phys. Lett., **80**, pp. 497–499.
[8] Dais, C., Solak, H. H., Müller, E., and Grützmacher, D., 2008, "Impact of Template Variations on Shape and Arrangement of Si/Ge Quantum Dot Arrays," Appl. Phys. Lett., **92**, p. 143102.
[9] Lu, W., and Suo, Z., 2001, "Dynamics of Nanoscale Pattern Formation of an Epitaxial Monolayer," J. Mech. Phys. Solids, **49**, pp. 1937–1950.
[10] Lu, W., and Kim, D., 2004, "Patterning Nanoscale Structures by Surface Chemisty," Nano Lett., **4**, pp. 313–316.
[11] Kukta, R. V., and Kouris, D., 2005, "On the Mechanisms of Epitaxial Island Alignment on Patterned Substrates," J. Appl. Phys., **97**, p. 033527.
[12] Machtay, N. D., and Kukta, R. V., 2006, "Energetics of Epitaxial Island Arrangements on Substrate Mesas," ASME J. Appl. Mech., **73**, pp. 212–219.
[13] Liu, P., Zhang, Y.-W., Lu, C., and Lam, K.-Y., 2008, "Three-Dimensional Analysis of the Guided-Assembled Growth of Heteroepitaxial Islands on Imperfectly Pre-Patterned Surfaces," Nanotechnology, **19**, p. 185302.
[14] Pan, E., Sun, M., Chung, P. W., and Zhu, R., 2007, "Three-Dimensional Kinetic Monte Carlo Simulation of Prepatterned Quantum-Dot Island Growth," Appl. Phys. Lett., **91**, p. 193110.
[15] Liu, P., Zhang, Y. W., and Lu, C., 2007, "Phase Diagrams for Growing Ordered Heteroepitaxial Quantum Dots and Quantum Rings by Surface Prepatterning," Appl. Phys. Lett., **90**, p. 071905.
[16] Chiu, C.-H., and Huang, Z., 2007, "Numerical Simuation for the Formation of Nanostructures on the Stranski-Krastanow Systems by Surface Undulation," J. Appl. Phys., **101**, p. 113540.
[17] Levine, M. S., Golovin, A. A., Davis, S. H., and Voorhees, P. W., 2007, "Self-Assembly of Quantum Dots in a Thin Epitaxial Film Wetting an Elastic Substrate," Phys. Rev. B, **75**, p. 205312.
[18] Kukta, R. V., and Bhattacharya, K., 2002, "A Micromechanical Model of Surface Steps," J. Mech. Phys. Solids, **50**, pp. 615–649.
[19] Kukta, R. V., Peralta, A., and Kouris, D., 2002, "Elastic Interaction of Durface Steps: Effect of Atomic-Scale Roughness," Phys. Rev. Lett., **88**, p. 186102.
[20] Shchukin, V. A., Ledentsov, N. N., Kop'ev, P. S., and Bimberg, D., 1995, "Spontaneous Ordering of Arrays of Coherent Strained Islands," Phys. Rev. Lett., **75**(16), pp. 2968–2971.
[21] Tambe, D. T., and Shenoy, V. B., 2004, "On the Energetic Origin of Self-Limiting Trenches Formed Around Ge/Si Quantum Dots," Appl. Phys. Lett., **85**, pp. 1586–1588.
[22] Denker, U., Schmidt, O., Jin-Philipp, N.-Y., and Eberl, K., 2001, "Trench Formation Around and Between Self-Assembled Ge Islands on Si," Appl. Phys. Lett., **78**, pp. 3723–3725.